

# Effects of growth pressure on erbium doped GaN infrared emitters synthesized by metal organic chemical vapor deposition

I-Wen Feng,<sup>1,\*</sup> Jing Li,<sup>1</sup> Jingyu Lin,<sup>1</sup> Hongxing Jiang,<sup>1</sup>  
and John Zavada<sup>2</sup>

<sup>1</sup>Department of Electrical & Computer Engineering, Texas Tech University, Lubbock, TX 79409, USA

<sup>2</sup>Department of Electrical & Computer Engineering, Polytechnic Institute of New York University,  
New York, NY 11201, USA

\*i-wen.feng@ttu.edu

**Abstract:** Er doped GaN (GaN:Er) p-i-n structures were prepared by metal organic chemical vapor deposition. Effects of growth pressure on the optical performance of GaN:Er p-i-n structures have been investigated. Electroluminescence measurements revealed that the optimal growth pressure window for obtaining strong infrared emission intensity at 1.54  $\mu\text{m}$  is around 20 torr, while the greater amount of Ga vacancies or non-radiative transitions were observed from the ones grown at lower or higher pressure. Our results point to possible applications in optical communications using current injected optical amplifiers based on GaN:Er p-i-n structures.

©2012 Optical Society of America

OCIS codes: (160.5690) Rare-earth-doped materials; (230.3670) Light-emitting diodes.

---

## References and links

1. R. Birkhahn and A. J. Steckl, "Green emission from Er-doped GaN grown by molecular beam epitaxy on Si substrates," *Appl. Phys. Lett.* **73**(15), 2143–2145 (1998).
2. A. J. Steckl, M. Garter, R. Birkhahn, and J. Scofield, "Green electroluminescence from Er-doped GaN Schottky barrier diodes," *Appl. Phys. Lett.* **73**(17), 2450–2452 (1998).
3. R. Dahal, J. Y. Lin, H. X. Jiang, and J. M. Zavada, "Er-doped GaN and  $\text{In}_x\text{Ga}_{1-x}\text{N}$  for optical communication," in *Rare-Earth Doped III-Nitrides for Optoelectronic and Spintronic Applications*, K. P. O'Donnell and V. Dierolf, eds. (Springer, the Netherlands, 2010).
4. A. A. Saleh, R. M. Jopson, J. D. Evankow, and J. Aspell, "Modeling of gain in erbium-doped fiber amplifiers," *IEEE Photon. Technol. Lett.* **2**(10), 714–717 (1990).
5. A. Koizumi, Y. Fujiwara, A. Urakami, K. Inoue, T. Yoshikane, and Y. Takeda, "Room-temperature electroluminescence properties of Er, O-codoped GaAs injection-type light-emitting diodes grown by organometallic vapor phase epitaxy," *Appl. Phys. Lett.* **83**(22), 4521–4523 (2003).
6. S. Wang, A. Eckau, E. Neufeld, R. Carius, and C. Buchal, "Hot electron impact excitation cross-section of Er and electroluminescence from erbium-implanted silicon metal-oxide-semiconductor tunnel diodes," *Appl. Phys. Lett.* **71**(19), 2824–2826 (1997).
7. J. T. Torvik, C. H. Qiu, R. J. Feuerstein, J. I. Pankove, and F. Namavar, "Photo-, cathodo-, and electroluminescence from erbium and oxygen co-implanted GaN," *J. Appl. Phys.* **81**(9), 6343–6350 (1997).
8. C. Ugolini, N. Nepal, J. Y. Lin, H. X. Jiang, and J. M. Zavada, "Erbium-doped GaN epilayers synthesized by metal-organic chemical vapor deposition," *Appl. Phys. Lett.* **89**(15), 151903 (2006).
9. Q. Wang, R. Hui, R. Dahal, J. Y. Lin, and H. X. Jiang, "Carrier lifetime in erbium-doped GaN waveguide emitting in 1540 nm wavelength," *Appl. Phys. Lett.* **97**(24), 241105 (2010).
10. C. Ugolini, N. Nepal, J. Y. Lin, H. X. Jiang, and J. M. Zavada, "Excitation dynamics of the 1.54  $\mu\text{m}$  emission in Er doped GaN synthesized by metal organic chemical vapor deposition," *Appl. Phys. Lett.* **90**(5), 051110 (2007).
11. T. C. Banwell and A. Jayakumar, "Exact analytical solution for current flow through diode with series resistance," *Electron. Lett.* **36**(4), 291–292 (2000).
12. P. Barnes and T. Paoli, "Derivative measurements of the current-voltage characteristics of double-heterostructure injection lasers," *IEEE J. Quantum Electron.* **12**(10), 633–639 (1976).
13. B. Heying, X. H. Wu, S. Keller, Y. Li, D. Kapolnek, B. P. Keller, S. P. DenBaars, and J. S. Speck, "Role of threading dislocation structure on the x-ray diffraction peak widths in epitaxial GaN films," *Appl. Phys. Lett.* **68**(5), 643–645 (1996).

14. R. Heitz, P. Thurian, I. Loa, L. Eckey, A. Hoffmann, I. Broser, K. Pressel, B. K. Meyer, and E. N. Mokhov, "Identification of the 1.19-eV luminescence in hexagonal GaN," *Phys. Rev. B Condens. Matter* **52**(23), 16508–16515 (1995).
15. J. Baur, U. Kaufmann, M. Kunzer, J. Schneider, H. Amano, I. Akasaki, T. Detchprohm, and K. Hiramatsu, "Photoluminescence of residual transition metal impurities in GaN," *Appl. Phys. Lett.* **67**(8), 1140–1142 (1995).
16. J. Baur, K. Maier, M. Kunzer, U. Kaufmann, J. Schneider, H. Amano, I. Akasaki, T. Detchprohm, and K. Hiramatsu, "Infrared luminescence of residual iron deep level acceptors in gallium nitride (GaN) epitaxial layers," *Appl. Phys. Lett.* **64**(7), 857–859 (1994).
17. A. Sedhain, J. Li, J. Y. Lin, and H. X. Jiang, "Nature of deep center emissions in GaN," *Appl. Phys. Lett.* **96**(15), 151902 (2010).
18. R. Wang and A. J. Steckl, "Effect of Si and Er co-doping on green electroluminescence from GaN:Er ELDs," in *MRS Proceedings* (2008), Vol. 1068, p. 1068–C05–03.

## 1. Introduction

Erbium (Er) is one of the rare earth elements whose intra- $4f$  transitions have been extensively researched due to their potential applications. Intra- $4f$  transitions include the green emissions at 537 nm and 558 nm (transitions from  $^2H_{11/2}$  to  $^4I_{15/2}$  and from  $^4S_{3/2}$  to  $^4I_{15/2}$  state) for display applications and 1.54  $\mu\text{m}$  emission (transition from  $^4I_{13/2}$  to  $^4I_{15/2}$  state) for optical communications and other optoelectronic device applications [1–3]. In particular, the infrared emission at 1.54  $\mu\text{m}$ , which overlaps with the minimum optical loss band of silica fibers, has been greatly utilized in erbium doped fiber amplifiers (EDFA) for optical communications. While conventional EDFAs are optically pumped with pumping lasers either at 980 nm or 1480 nm [4], electrically pumped infrared emitters or optical amplifiers based on Er-doped semiconductors potentially offer compact, rugged components for high speed photonic integrated circuits. Previous studies have suggested that Er $^{3+}$  electroluminescence possesses larger excitation cross-section than Er $^{3+}$  photoluminescence pumped at resonant wavelength [5–7]. Among various host materials, the wide energy bandgap of III-nitride semiconductor materials reduces thermal quenching and leads to better room temperature performance [8]. In addition, the millisecond lifetime of the 1.54  $\mu\text{m}$  emissions [9] and the excellent crystalline quality of III-nitride epilayers make Er-doped III-nitride semiconductors promising candidates to serve as a new class of infrared emitters and optical amplifiers with minimal crosstalk for chip-scale applications.

Considerable efforts have been dedicated to the synthesis of Er-doped III-nitride materials, including ion implantation [7], molecular beam epitaxy (MBE) [2], and metal organic chemical vapor deposition (MOCVD). In our previous studies, we demonstrated the strong 1.54  $\mu\text{m}$  emission obtained from MOCVD grown Er-doped GaN (GaN:Er) semiconductors [8–10]. Most Er precursors used in MOCVD synthesis have much lower vapor pressures compared to other metal-organic precursors. This low vapor pressure of Er precursors limits the growth pressure of Er doped III-nitride materials, and hence causes crystalline imperfections including dislocations and defects. In this report, we prepared GaN:Er p-i-n structures by MOCVD with GaN:Er active layers grown under different pressures. The GaN:Er growth pressure was found to strongly affect the performance of GaN:Er p-i-n infrared emitters.

## 2. Growth and fabrication

A semi-insulating GaN:Er epilayer of 0.5  $\mu\text{m}$  in thickness was first grown at 1020  $^{\circ}\text{C}$  by MOCVD on an n-Al $_{0.75}$ Ga $_{0.25}$ N/AlN/Al $_2$ O $_3$  template. This was then followed by the growth of a GaN:Mg epilayer of 0.3  $\mu\text{m}$  in thickness to complete GaN:Er p-i-n infrared emitter structure, as shown in Fig. 1. The growth pressure of the semi-insulating GaN:Er epilayer of 0.5  $\mu\text{m}$  in thickness was varied from 10, 20, 30, to 40 torr. Trimethylgallium (TMGa), biscyclopentadienyl-magnesium (Cp $_2$ Mg), tris-isopropylcyclopentadienylerbium (TRIPeR), and ammonia (NH $_3$ ) were used as group-III, Mg-dopant, Er-dopant, and group-V precursors, respectively, and carried into the reactor by H $_2$  gas. The post-growth annealing process was performed at 550  $^{\circ}\text{C}$  in air ambient for 30 minutes to activate Mg acceptors in GaN:Mg layer.

Chloride-based inductively coupled plasma was used to etch the layers down to n-Al<sub>0.75</sub>Ga<sub>0.25</sub>N (Si-doped) layer, ~0.9 μm from the top of p-GaN:Mg surface. Ni/Au (30nm/120nm) contacts were deposited on top of p-type GaN:Mg layers as p-contact layers by e-beam evaporator, and then annealed at 550 °C in air ambient for 1 minute to attain Ohmic contacts. Finally, Ti/Al (30nm/120nm) contacts were deposited on n-Al<sub>0.75</sub>Ga<sub>0.25</sub>N layers to form n-contact layers. The crystalline, optical, and electrical properties of the GaN:Er p-i-n structures were analyzed by X-ray diffraction (XRD), NIR spectrometry, and micro-probing measurements.

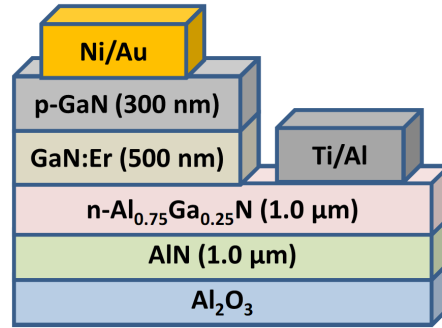


Fig. 1. Schematic diagram of the MOCVD grown GaN:Er p-i-n emitter structure used in this study.

### 3. Electrical and crystalline properties

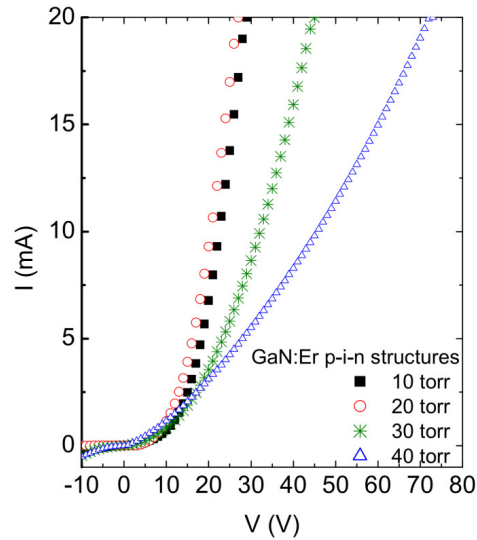


Fig. 2. I-V characteristics of GaN:Er p-i-n structures grown at different growth pressures from 10 to 40 torr.

The current-voltage (I-V) characteristics of the GaN:Er p-i-n structures are illustrated in Fig. 2, which can be described by Eq. (1), where  $I_{sat}$ ,  $R$ , and  $\eta$  refer to the saturation current, the series resistance, and the diode characteristic factor, respectively [11,12]:

$$I = I_{sat} \exp\left(\frac{q(V - IR)}{\eta kT} - 1\right). \quad (1)$$

When the applied current on the p-i-n structure is much higher than the saturation current ( $I \gg I_{\text{sat}}$ ), this I-V relationship can be simplified to estimate the series resistances of GaN:Er p-i-n structures using

$$I \frac{dV}{dI} = RI + \frac{\eta kT}{q}. \quad (2)$$

The full-width at half maxima (FWHM) of rocking curves (XRD  $\omega$ -scans) of the (002) reflection peak in GaN generally signify the crystalline qualities of GaN epilayers [13]. Rocking curves of  $\omega$ -scans of the (002) reflections from GaN:Er were measured and the results for four different growth pressures are illustrated in Fig. 3. The estimated series resistances and the values of FWHM in GaN:Er (002) rocking curves of these p-i-n structures are listed in Table 1. The observed general trend is that increasing the growth pressure of GaN:Er active layer leads to a broader GaN:Er (002) XRD rocking curve and also larger series resistances. This indicates that increasing growth pressure may have introduced more crystalline dislocations. These crystalline imperfections may deteriorate the electrical properties of the top p-type GaN:Mg layers, and hence contributed to the higher series resistances found in GaN:Er p-i-n structures grown at higher GaN:Er growth pressures. However, the effects on the I-V characteristics due to increased growth pressure are not significant for growth pressure  $\leq 20$  torr.

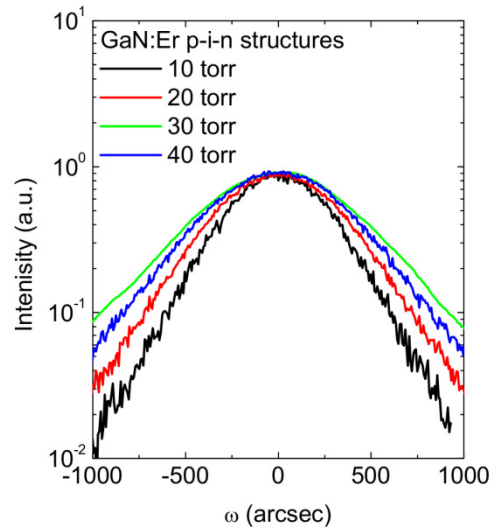


Fig. 3. GaN:Er (002) XRD rocking curves of the GaN:Er p-i-n structures with varying GaN:Er growth pressures from 10 to 40 torr.

**Table 1. Summary of parameters of GaN:Er p-i-n structures grown under different GaN:Er growth pressures (P); FWHM of GaN:Er (002) XRD rocking curves; and the estimated series resistance (R).**

P (Torr)	FWHM (arcsec)	R (k $\Omega$ )
10	670	0.36
20	740	0.40
30	830	1.01
40	800	1.23

#### 4. Optical properties

Electroluminescence properties of GaN:Er p-i-n emitter structures were measured. Infrared spectra shown in Fig. 4 were detected at 20 mA current injection from GaN:Er p-i-n structures grown at different GaN:Er growth pressures. The observed emission at 1.00  $\mu\text{m}$  ( $\sim 1.24$  eV) originates from the intra- $4f$  transition from  $^4I_{11/2}$  to  $^4I_{15/2}$  state of  $\text{Er}^{3+}$  atoms, while the emission at 1.54  $\mu\text{m}$  ( $\sim 0.81$  eV) is related to the transition from  $^4I_{13/2}$  to  $^4I_{15/2}$  state. The sample grown under 10 torr showed exceptionally strong emission at 1.05  $\mu\text{m}$  ( $\sim 1.19$  eV), about three times stronger than the 1.54  $\mu\text{m}$  emission detected from the same sample. The narrow line-width ( $\sim 13$  meV) of 1.05  $\mu\text{m}$  emission excludes the possibility of defect-level related transitions. This 1.05  $\mu\text{m}$  emission have also been previously found in some MOCVD-grown GaN epilayers, and has been reported as  $3d$ - $3d$  transitions of the unintentionally doped transition metals ( $\text{Cr}^{4+}$  or  $\text{Ti}^{2+}$ ) [14–16]. While increasing GaN:Er growth pressure from 10 to 20 torr, the 1.05  $\mu\text{m}$  emission was significantly decreased, and the 1.54  $\mu\text{m}$  emission was increased by almost one order of magnitude. The emission at 1.00  $\mu\text{m}$  is also increased but not as much. While further increasing GaN:Er growth pressure to 40 torr, the total intensity of the near infrared emissions dropped dramatically. The results thus indicate that high GaN:Er growth pressure ( $> 20$  torr) decreases the crystalline quality of the p-i-n structures and also introduces significant amount of non-radiative recombination centers.

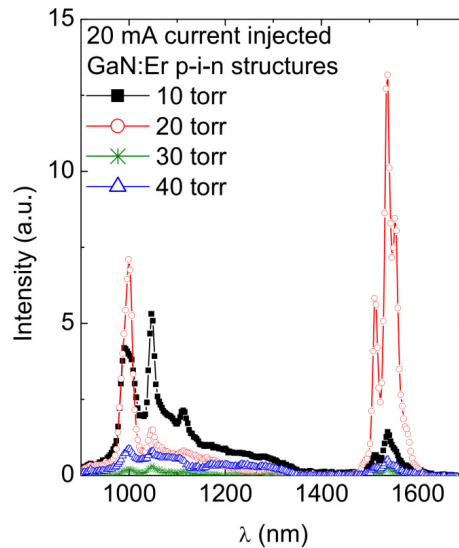


Fig. 4. Infrared spectra detected at 20 mA from GaN:Er p-i-n structures grown at different GaN:Er growth pressures from 10 to 40 torr. For GaN:Er growth pressure above 20 torr, the infrared emission intensity decreases significantly.

To investigate the underlying mechanism behind the variations in infrared emissions, two GaN p-i-n samples were grown without Er doping at 10 and 20 torr with the same growth parameters as the Er doped GaN:Er p-i-n structures. Figure 5 displays infrared spectra, at 20 mA current injection, obtained from these two GaN p-i-n structures without Er doping. One broad defect-related emission centered at 1.22 eV with a line-width of 230 meV was observed, and its intensity significantly decreased with an increase of GaN growth pressure. This broad infrared emission has been previously reported as a band-to-impurity transition related to the complexes of Ga vacancy and oxygen substitution on nitrogen site ( $V_{\text{Ga}}\text{-O}_{\text{N}}$ ) [17]. This  $V_{\text{Ga}}$  related transition, with energy close to 1.19 eV, could stimulate the narrow infrared emission line at 1.05  $\mu\text{m}$ . This would explain why, as GaN:Er growth pressure

increases, the intensity of 1.05  $\mu\text{m}$  emission decreases, and the 1.54  $\mu\text{m}$  emission becomes stronger. Under forward bias, the intra- $4f$  transitions of  $\text{Er}^{3+}$  are predominantly induced by the energy transfer from the electron-hole pairs generated through band edge excitation via current injection [18]. The results suggest that the competitive non-radiative recombination rate increased due to the formation of more impurities and defects under low growth pressure (<10 torr) or high growth pressure (>30 torr), which may limit the number of excited  $\text{Er}^{3+}$  centers and hence the 1.54  $\mu\text{m}$  emission.

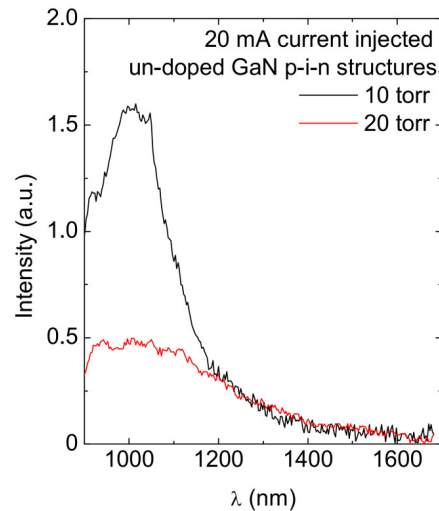


Fig. 5. Infrared spectra detected at 20 mA from GaN p-i-n structures without Er-doping grown at two GaN growth pressures of 10 and 20 torr.

## 5. Conclusions

In summary, the 1.54  $\mu\text{m}$  emission from GaN:Er p-i-n structures was significantly enhanced by increasing GaN:Er growth pressure from 10 to 20 torr. This is possibly due to fewer Ga vacancy related defects generated under higher GaN:Er growth pressure, which results in reduced number of competitive recombination defects or impurities. Further increase in GaN:Er growth pressure reduces the infrared emission due to increased crystalline dislocations. The strong emission at 1.54  $\mu\text{m}$  points to possible applications in optical communications using current injected optical amplifiers based on GaN:Er p-i-n structures.

## Acknowledgments

This work is supported by a grant from NSF (ECCS-0854619 and ECCS-1200168). HXJ and JYL thank the AT&T Foundation for the support of Ed Whitacre and Linda Whitacre endowed chairs. JZ acknowledges support from NSF under the IR/D program.